

# Investigation of the Binding of Fluorolumazines to the 1-MDa Capsid of Lumazine Synthase by $^{15}\text{N}\{^{19}\text{F}\}$ REDOR NMR

Jon M. Goetz,<sup>†</sup> Barbara Poliks,<sup>‡</sup> Daniel R. Studelska,<sup>†</sup> Markus Fischer,<sup>§</sup> Karl Kugelbrey,<sup>§</sup> Adelbert Bacher,<sup>§</sup> Mark Cushman,<sup>\*,||</sup> and Jacob Schaefer<sup>\*,†</sup>

Contribution from the Department of Chemistry, Washington University, Saint Louis, Missouri 63130, Department of Physics, State University of New York at Binghamton, Binghamton, New York 13902, Lehrstuhl für Organische Chemie und Biochemie, Technische Universität München, D-85747 Garching, Germany, and Department of Medicinal Chemistry and Molecular Pharmacology, School of Pharmacy, Purdue University, West Lafayette, Indiana 47907

Received October 30, 1998. Revised Manuscript Received June 11, 1999

**Abstract:** The  $^{15}\text{N}\{^{19}\text{F}\}$  REDOR NMR spectra of two fluorolumazines complexed to the 1-MDa  $\beta_{60}$  capsid of lumazine synthase have been obtained at 20.3 and 50.7 MHz. Distances from  $\text{CF}_3$  groups of the ligands to six side- and main-chain nitrogens have been measured. These distances were used in combination with the X-ray crystal coordinates of wild-type lumazine synthase, complexed to a related substrate ligand, in a series of distance-restrained molecular dynamics simulations. The result is a model of the binding site of lumazine synthase that has sufficient detail to predict the absolute configuration at C-7 of complexed 7-hydroxy-8-D-ribose-1,6,7-bis(trifluoromethyl)-7,8-dihydropteridine-2,4(1*H*,3*H*)-dione, a fluorinated analogue of an unstable, hypothetical intermediate in the reactions catalyzed by both lumazine synthase and riboflavin synthase.

## Introduction

Heavy riboflavin synthase of *Bacillus subtilis* contains three  $\alpha$  subunits (23 kDa) and sixty  $\beta$  subunits (16 kDa) to form an  $\alpha_3\beta_{60}$  complex that catalyzes the biosynthesis of riboflavin (Scheme 1). The enzymes of riboflavin biosynthesis are present in a number of microorganisms but not in mammals.<sup>1–7</sup> These enzymes are therefore potential targets for antibiotics, and structural details of inhibitors in the  $\alpha_3\beta_{60}$  binding sites could therefore lead to templates for the design of effective drugs. The  $\beta$  subunits are involved with the formation of lumazine **3** and the  $\alpha$  subunits with the formation of riboflavin (**4**). In the full complex, the  $\alpha$  subunits are secluded in the center of an approximately spherical capsid formed by the sixty  $\beta$  subunits.<sup>8–13</sup> The 1-MDa  $\beta_{60}$  enzyme complex retains activity<sup>9</sup> and so

characterization of this binding site has relevance for an understanding of those of  $\alpha_3\beta_{60}$ . The X-ray structure of the icosahedral  $\beta_{60}$  capsid in the heavy riboflavin synthase of *Bacillus subtilis* ( $\alpha_3\beta_{60}$  complex) with a bound substrate analogue has been determined at 3.3-Å resolution.<sup>8</sup> In addition, a more recent X-ray structure of the reconstituted, hollow  $\beta_{60}$  capsid with a bound substrate analogue is available at 2.4-Å resolution.<sup>10</sup>

Our strategy to determine a higher resolution structure of occupied binding sites of lumazine synthase is to refine the relatively low-resolution X-ray information using REDOR NMR.<sup>14–20</sup> Well-resolved  $^{15}\text{N}$  solid-state NMR signals are generally observed for histidine, arginine, and lysine side chain nitrogens of uniformly  $^{15}\text{N}$ -labeled proteins.<sup>21</sup> It is therefore possible to measure accurately a few specific distances from fluorines of product-analogue ligands to nitrogens of the uniformly  $^{15}\text{N}$ -labeled protein. For example, from the X-ray structure we know that of the 9 lysines in each  $\beta$  subunit, only

<sup>†</sup> Washington University.

<sup>‡</sup> State University of New York.

<sup>§</sup> Technische Universität München.

<sup>||</sup> Purdue University.

(1) Plaut, G. W. E.; Smith, C. M.; Alworth, W. L. *Annu. Rev. Biochem.* **1974**, *43*, 899–922.

(2) Plaut, G. W. E. In *Comprehensive Biochemistry*; Florin M., Stotz, E. H., Eds.; Elsevier: Amsterdam, 1971; Vol. 21, pp 11–45.

(3) Brown, G. M.; Williamson, J. M. In *Escherichia coli and Salmonella typhimurium*; Neidhardt, F. C., Ingraham, J. L., Low, K. B., Magasanik, B., Schaechter, M., Umberger, H. E., Eds.; American Society for Microbiology: Washington, DC, 1987; p 521.

(4) Bacher, A.; Ladenstein, R. In *Chemistry and Biochemistry of Flavoenzymes*; Müller, F., Ed.; Chemical Rubber Co.: Boca Raton, FL, 1991; Vol. II, pp 293–316.

(5) Bacher, A.; Fischer, M.; Kis, K.; Kugelbrey, K.; Mörtl, S.; Scheuring, J.; Weinkauff, S.; Eberhardt, S.; Schmidt-Bäse, K.; Huber, R.; Ritsert, K.; Cushman, M.; Ladenstein, R. *Biochem. Soc. Trans.* **1996**, *24*, 89–94.

(6) Kis, K.; Volk, R.; Bacher, A. *Biochemistry* **1995**, *34*, 2883–2892.

(7) Kis, K.; Bacher, A. *J. Biol. Chem.* **1995**, *270*, 16788–16795.

(8) Ladenstein, R.; Schneider, M.; Huber, R.; Bartunik, H. D.; Wilson, K.; Schott, K.; Bacher, A. *J. Mol. Biol.* **1988**, *203*, 1045–1070.

(9) Bacher, A.; Eisenreich, W.; Kis, K.; Ladenstein, R.; Richter, G.; Scheuring, J.; Weinkauff, S. In *Bioorganic Chemistry Frontiers*; Dugas, H., Schmidtchen, F. P., Eds.; Springer-Verlag: Berlin, 1993; Vol. 3, pp 147–192.

(10) Ritsert, K.; Huber, R.; Turk, D.; Ladenstein, R.; Schmidt-Bäse, K.; Bacher, A. *J. Mol. Biol.* **1995**, *253*, 151–167.

(11) Bacher, A.; Ludwig, H. C.; Schnepfle, H.; Ben-Shaul, Y. *J. Mol. Biol.* **1986**, *187*, 75–86.

(12) Ladenstein, R.; Meyer, B.; Huber, R.; Labischinski, H.; Bartels, K.; Bartunik, H.-D.; Bachman, L.; Ludwig, H. C.; Bacher, A. *J. Mol. Biol.* **1986**, *187*, 87–100.

(13) Ladenstein, R.; Ritsert, K.; Richter, G.; Bacher, A. *Eur. J. Biochem.* **1994**, *223*, 1007–1017.

(14) Gullion, T.; Schaefer, J. *J. Magn. Reson.* **1989**, *81*, 196–200.

(15) Gullion, T.; Schaefer, J. *Adv. Magn. Reson.* **1989**, *13*, 57–81.

(16) Wang, J.; Balazs, Y. S.; Thompson, L. K. *Biochemistry* **1997**, *36*, 1699–1703.

(17) Garbow, J. R.; Breslav, M.; Antohi, O.; Naider, F. *Biochemistry* **1994**, *33*, 10094–10099.

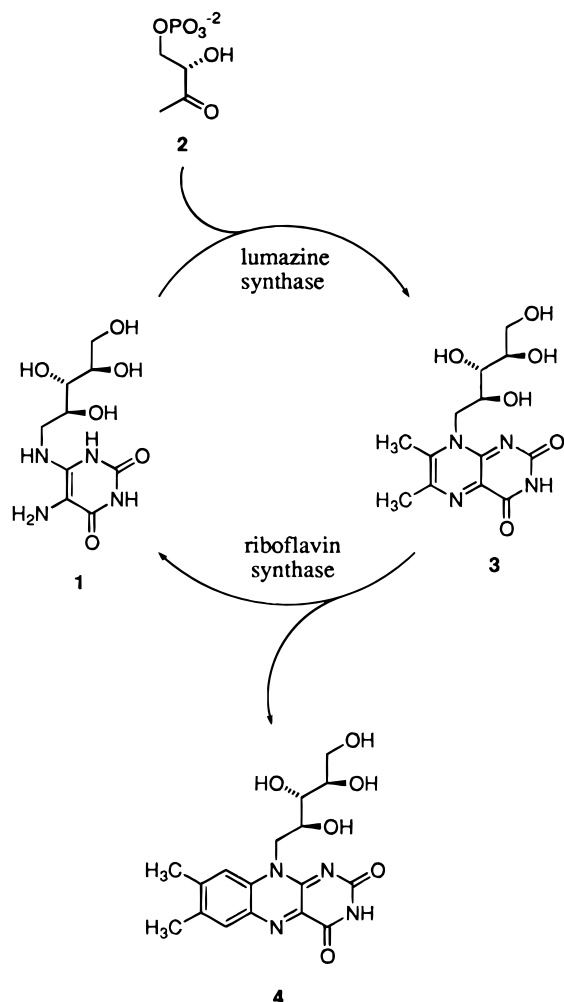
(18) Li, Y.; Appleyard, R. J.; Shuttleworth, W. A.; Evans, J. N. S. *J. Am. Chem. Soc.* **1994**, *116*, 10799–10800.

(19) Jakeman, D. L.; Mitchell, D. J.; Shuttleworth, W. A.; Evans, J. N. S. *Biochemistry* **1998**, *37*, 12012–12019.

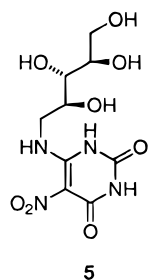
(20) Michal, C. A.; Jelinski, L. W. *J. Biomol. NMR* **1998**, *12*, 231–241.

(21) Hing, A. W.; Tjandra, N.; Cottam, R. F.; Schaefer, J.; Ho, C. *Biochemistry* **1994**, *33*, 8651–8661.

Scheme 1

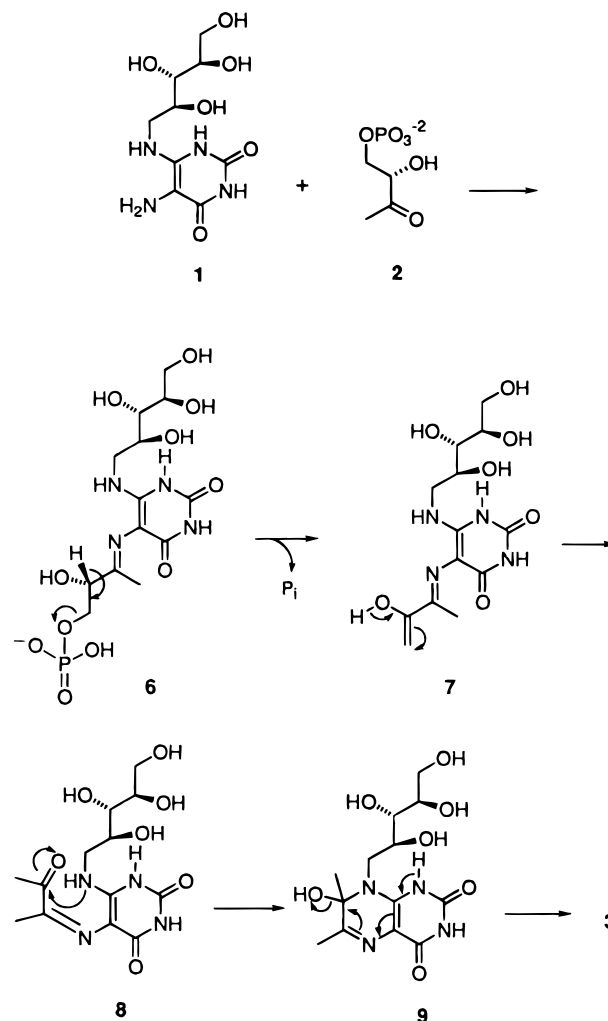


one is in the vicinity of the binding site. Thus, a REDOR determination of the distance of the  $\epsilon$ - $^{15}\text{N}$  of this lysine side chain nitrogen to the  $^{19}\text{F}$  of the ligand (which for N–F distances of the order of 5 Å is possible to within  $\pm 0.2$  Å)<sup>21</sup> is much more accurate than the corresponding distance determination from X-ray analysis alone. Additional accurate distances can be determined by  $^{15}\text{N}\{^{19}\text{F}\}$  REDOR from ligand fluorines to histidine and arginine side chain nitrogens identified as proximate by the X-ray structure. A refined structure of the liganded binding site of the  $\beta_{60}$  capsid is then generated from a molecular dynamics simulation starting with the X-ray coordinates and restrained by the REDOR-determined distances.



The design of suitable  $^{19}\text{F}$ -containing ligands for lumazine synthase was based on the X-ray structure of the  $\beta_{60}$  capsid and consideration of the mechanism of the enzyme-catalyzed reaction (Scheme 2).<sup>5,10,13</sup> The X-ray structure has provided a description of the active site occupied by the substrate analogue

Scheme 2



5-nitro-6-(D-ribitylamino)-2,4-(1H,3H)pyrimidinedione (5), although the 2.4 Å resolution leaves details of the bound ligand conformation unclear. In addition to the X-ray structure, the identification of the four-carbon precursor 2 was made unambiguously.<sup>22–24</sup> With the identities of both of the substrates 1 and 2 known, steady-state enzyme kinetic parameters for recombinant  $\beta_{60}$  capsids devoid of  $\alpha$  subunits were measured,<sup>6,7</sup> and inhibition constants of potential lumazine synthase inhibitors were determined.<sup>23,24</sup>

A hypothetical mechanism for the  $\beta$  subunit-catalyzed reaction is shown in Scheme 2.<sup>22</sup> According to this proposal, the initial step involves Schiff base formation between the more reactive amino group of 1 and the ketone 2. Elimination of phosphate from the Schiff base 6 yields the enol 7, which tautomerizes to the ketone 8. Nucleophilic attack of the secondary amine on the ketone carbon atom of 8 then affords the carbinolamine 9, which eliminates water to form the lumazine 3.

As a prerequisite for the design of mechanism-based riboflavin synthase inhibitors, a working hypothesis was adopted for the riboflavin synthase-catalyzed reaction (Scheme 3).<sup>25–27</sup>

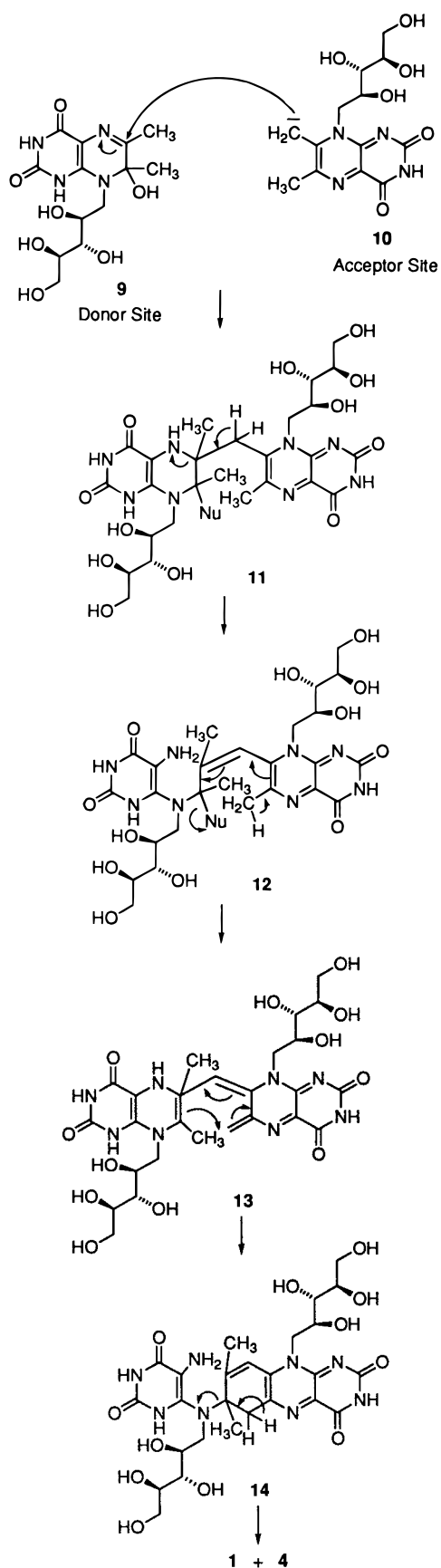
(22) Volk, R.; Bacher, A. *J. Am. Chem. Soc.* **1988**, *110*, 3651–3653.

(23) Cushman, M.; Mavandadi, F.; Kugelbrey, K.; Bacher, A. *Bioorg. Med. Chem.* **1998**, *6*, 409–415.

(24) Cushman, M.; Mavandadi, F.; Kugelbrey, K.; Bacher, A. *J. Org. Chem.* **1998**, *62*, 88944–8947.

(25) Beach, R. L.; Plaut, G. W. E. *J. Am. Chem. Soc.* **1970**, *92*, 2913–2916.

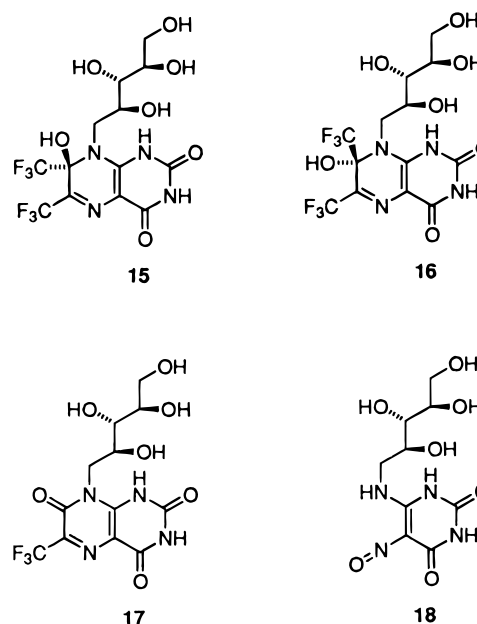
Scheme 3



In this proposal, the anion **10** formed by deprotonation of the C-7 methyl group of **3** at the acceptor site of the enzyme adds to the imine group of **9** at the donor site. Intermediate **9** is derived from **3** by covalent hydration. A 1,2-elimination in **11**

followed by a 1,6-elimination in **12** yields a conjugated triene system in **13**, which undergoes a 3,3-sigmatropic rearrangement to afford intermediate **14**. Intermediate **14** then aromatizes by 1,2-elimination to yield the final products, riboflavin (**4**) and the pyrimidinedione **1**.

Inspection of Schemes 2 and 3 reveals that the covalently hydrated lumazine **9** plays a key role in the reactions catalyzed by both lumazine synthase and riboflavin synthase. It is thought to be the last intermediate in the lumazine synthase-catalyzed reaction, and it is also proposed as an early intermediate in the riboflavin synthase-catalyzed reaction. To create an analogue of **9** having a stabilized covalently hydrated structure that might interact with both lumazine synthase as well as riboflavin synthase, the epimeric 6,7-bis(trifluoromethyl)-8-ribityllumazines **15** and **16** were synthesized.<sup>28</sup> Only one of these, which



we named "epimer A", bound to the light riboflavin synthase of *Bacillus subtilis*.<sup>28</sup> We assumed that the configuration at C-7 of epimer A is the same as that of the substrate molecule **9** bound at the donor site of riboflavin synthase. In addition, we found that epimer A, but not epimer B, was converted to 6-trifluoromethyl-7-oxo-8-ribityllumazine (**17**) in the presence of the lumazine synthase/riboflavin synthase complex at pH 6.8 and 4 °C.<sup>29</sup> Both epimers were able to bind to lumazine synthase.<sup>29</sup> Interestingly, the product **17** was found to be an inhibitor of riboflavin synthase, but in contrast to epimer A, which binds with a stoichiometry of one molecule per protein subunit, presumably at the donor site, two molecules of compound **17** are bound to each protein subunit, presumably at both the donor site and the acceptor site.<sup>27</sup> We also determined that the 7-oxo product **17** binds to lumazine synthase with a 1:1 stoichiometry and a  $K_D$  of approximately 100  $\mu\text{M}$  (unpublished results).

In this paper we report the results of  $^{15}\text{N}\{^{19}\text{F}\}$  REDOR NMR measurements of fluorine-containing **15** (epimer B) and inhibitor **17**, each bound to the 1-MDa  $\beta_{60}$  capsid of lumazine synthase.

(26) Paterson, T.; Wood, H. C. S. *J. Chem. Soc., Chem. Commun.* **1969**, 290–291.

(27) Cushman, M.; Patel, H.; Scheuring, J.; Bacher, A. *J. Org. Chem.* **1992**, *57*, 5630–5643.

(28) Cushman, M.; Patrick, D. A.; Bacher, A.; Scheuring, J. *J. Org. Chem.* **1991**, *56*, 4603–4608.

(29) Scheuring, J.; Cushman, M.; Bacher, A. *J. Org. Chem.* **1995**, *60*, 243–245.

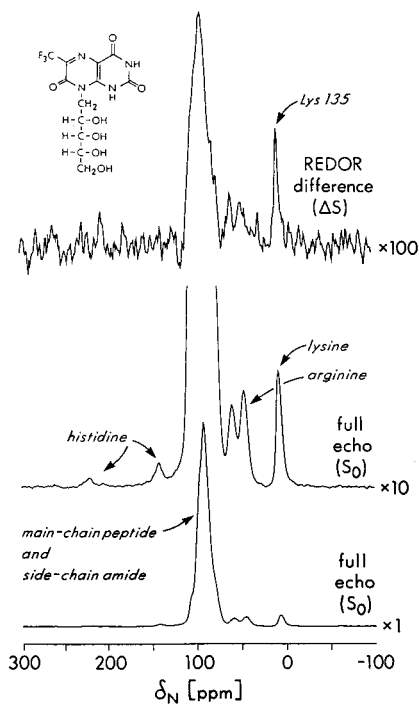


**Figure 1.** 20.3-MHz  $^{15}\text{N}\{^{19}\text{F}\}$  REDOR NMR spectra of 6-trifluoromethyl-7-oxo-8-ribityllumazine (**17**) complexed to [uniform- $^{15}\text{N}$ ]-F22W-lumazine synthase after 64 rotor cycles of dipolar evolution with magic-angle spinning at 5.000 kHz.

The reactive epimer B was complexed without degradation using low-temperature lyophilization.<sup>30</sup> REDOR-determined distances for both lyophilized complexes were restraints for molecular dynamics simulations that were based on the X-ray structure for the starting coordinates. The final result is a high-resolution structure of the lumazine synthase binding site determined by the combination of X-ray and REDOR analyses that is of higher quality than that determined by either method alone.

## Results and Discussion

**7-Oxo Product 17.** The 20.3-MHz  $^{15}\text{N}\{^{19}\text{F}\}$  REDOR spectra of **17** complexed to [uniform- $^{15}\text{N}$ ]-F22W-lumazine synthase are shown in Figure 1. There are 9 lysines, 5 arginines, and 2 histidines in the 16.2-kD lumazine synthase subunit, and resonances from all three of their side chain nitrogens are well resolved from one another in the full-echo spectrum (Figure 1, bottom). The ratio of peptide and amide integrated signal intensity (centered at 95 ppm) to the lysyl  $\epsilon$ - $^{15}\text{N}$  signal intensity (10 ppm) is 23:1, once laboratory and rotating-frame relaxation have been taken into account (data not shown). The theoretical ratio is 22:1. The close agreement means that all lysines are reporting for lumazine synthase, presumably because low-frequency motions are suppressed for the rigid capsid.

On the basis of the X-ray structure of the active site, only Lys135 of the 9 lysines in the subunit is proximate to the fluorinated **17**. Thus, the REDOR difference signal ( $\Delta S = S_0 - S$ , where  $S$  and  $S_0$  are echo intensities with and without dephasing pulses, respectively) at 10 ppm (Figure 1, top) is due exclusively to a single nitrogen. The REDOR ratio ( $S/S_0$ ) for this nitrogen reaches a minimum after 64 rotor cycles of dipolar evolution (with magic-angle spinning at 5 kHz), and then increases slightly for 96 rotor cycles of evolution (Figure 2). The increase indicates that full dephasing was achieved for the

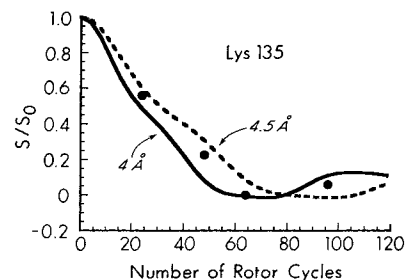


**Figure 2.** 20.3-MHz  $^{15}\text{N}\{^{19}\text{F}\}$  REDOR dephasing ( $S/S_0$ ) for the  $\epsilon$ -nitrogen of Lys135 of the complex of Figure 1.

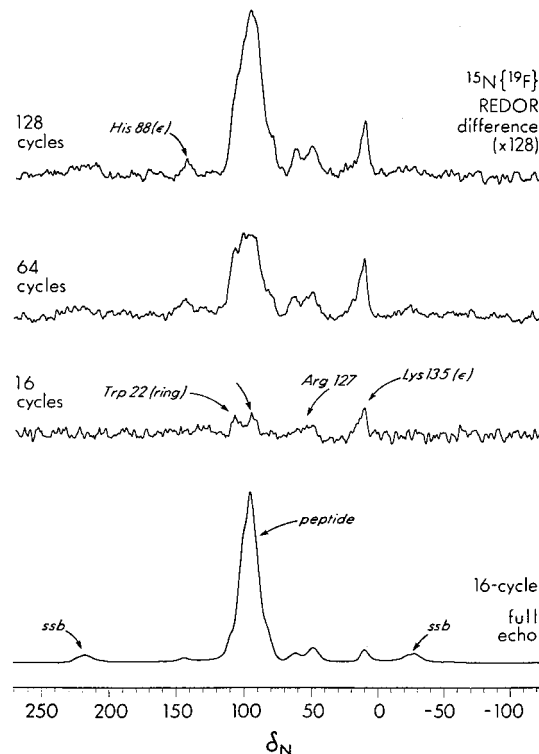


**Figure 3.** 50.7-MHz  $^{15}\text{N}\{^{19}\text{F}\}$  REDOR NMR spectra of 6-trifluoromethyl-7-oxo-8-ribityllumazine (**17**) complexed to [uniform- $^{15}\text{N}$ ]-F22W-lumazine synthase as a function of the number of rotor cycles of dipolar evolution. The full-echo spectrum at the bottom of the figure is for 16 rotor cycles.

$\text{CF}_3$ - $^{15}\text{N}$  group. The absolute level of this dephasing as measured by  $\Delta S/S_0$  is 0.08 (Figure 1) rather than  $1/8 = 0.12$ . This deviation is consistent with the expected occupancy of binding sites of approximately 75%, based on the  $136 \mu\text{M}$  concentration of both ligand and enzyme during formation of the complex, and a binding constant for **17** of approximately  $100 \mu\text{M}$ . The dephasing of Figure 2 has been adjusted to take into account the fact that 25% of the binding sites are empty by setting  $S/S_0 = 0$  for  $N_c = 64$ , and scaling the other values accordingly. Calculations matching the resulting adjusted dephasing indicate that the distance from the center of the  $\text{F}_3$  triangle to the  $\epsilon$ -nitrogen of Lys135 is  $4.2 \pm 0.2 \text{ \AA}$  (Figure 2).

The 50.7-MHz  $^{15}\text{N}\{^{19}\text{F}\}$  REDOR spectra of **17** complexed to [uniform- $^{15}\text{N}$ ]-F22W-lumazine synthase are shown in Figure 3. This sample was prepared so that all binding sites are occupied (see Experimental Section). The increased sensitivity of the 12-T spectrometer makes practical detection of weak difference signals in the 100-ppm region after just 16 rotor cycles of dipolar evolution, with magic-angle spinning at 6.250 kHz (Figure 3, second from bottom). The REDOR difference at 105 ppm is assigned to the indole ring nitrogen of Trp22,

(30) Studelska, D. R.; McDowell, L. M.; Espe, M. P.; Klag, C. A.; Schaefer, J. *Biochemistry* **1997**, *36*, 15555–15560.

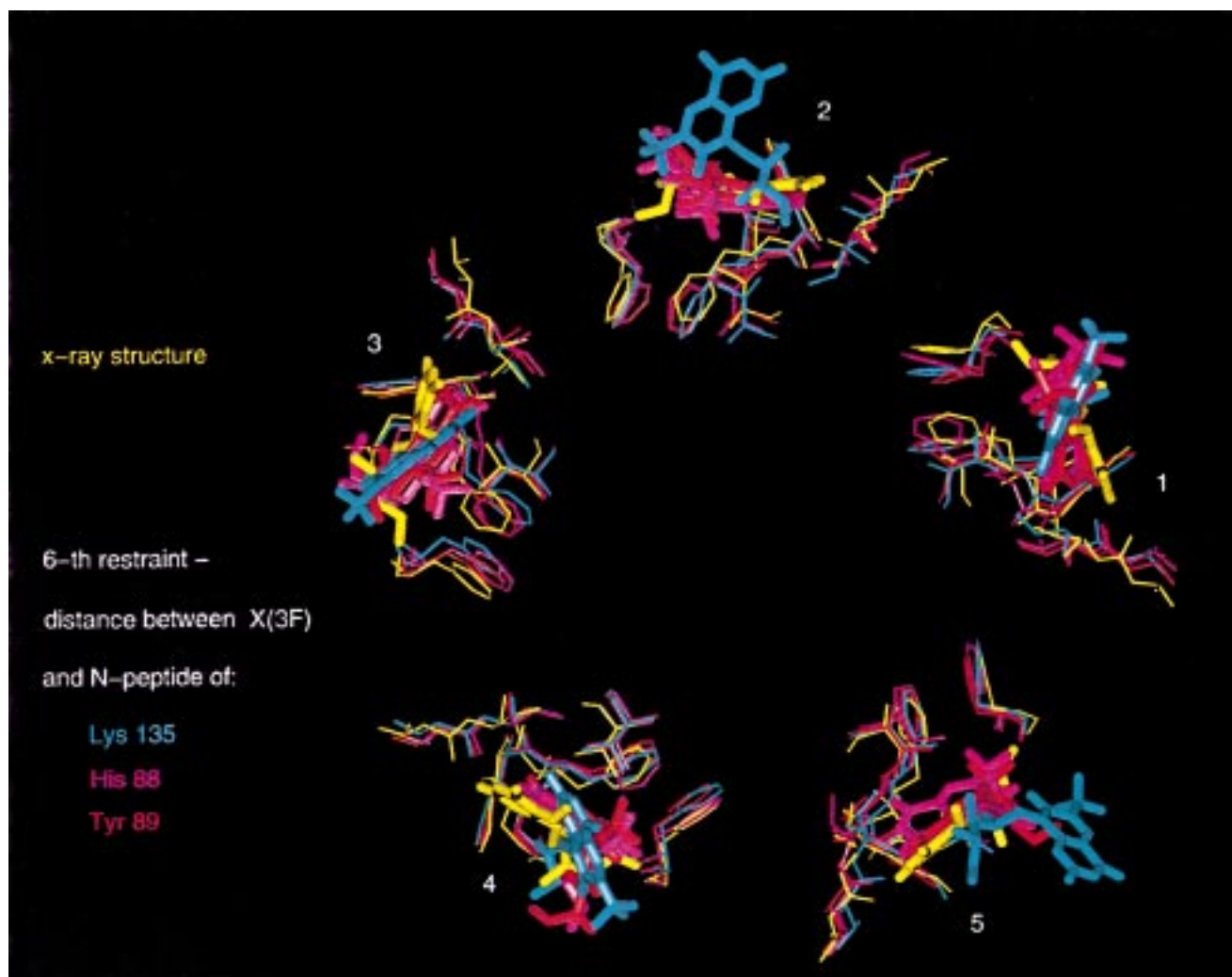


**Figure 4.** Models of the lumazine synthase binding site containing 6-trifluoromethyl-7-oxo-8-ribityllumazine (**17**). The models resulted from molecular dynamics simulations restrained by the five REDOR distances of Table 1. A sixth restraint was a 4.6-Å distance from the CF<sub>3</sub> of the ligand to N [of Lys135 (blue), His88 (purple), or Tyr89 (red)]. All residues are shown that have at least one atom within 3 Å of the ligand, which is itself highlighted.

which the X-ray structure puts in the vicinity of a bound substrate analogue. Replacing F22 by tryptophan in the F22W mutant did not affect the catalytic activity of the enzyme. Possibilities for the REDOR difference at 97 ppm include the  $\alpha$  nitrogens of Lys135, Tyr89, and His88. REDOR dephasing was also measured for  $N_c = 32, 64, 96,$  and  $128$  rotor cycles. Distances to the CF<sub>3</sub> group were determined for those nitrogens whose line assignments are unambiguous (see Figure 3). These values are presented in Table 1. The His88 restraint listed in the table was calculated to the protonated  $\epsilon$  ring nitrogen, which is four bonds from the  $\alpha$ -carbon atom.<sup>21</sup> High- and low-field distance measurements for the  $\epsilon$ -nitrogen of Lys135 are in agreement (Figure 2 and Table 1).

The three possibilities introduced by the uncertainty in the assignment of the signal at 97 ppm led to three different models of the binding of the ligand to the enzyme (Figure 4). These models were constructed by overlapping the structure of the ligand **17** with the nitroso ligand **18** in each of the five active sites surrounding a pentamer in the X-ray structure of lumazine synthase, followed by removal of **18**.<sup>8</sup> The structure then was relaxed slowly (with no REDOR restraints) with the convergence criterion of 1 kcal/(mol Å<sup>2</sup>). Afterward, a 20-ps molecular dynamics simulation with six REDOR restraints was performed, five of which are listed in Table 1. The sixth restraint was a distance of 4.6 Å to a backbone nitrogen, associated with the

**Table 1.** Distances Used as Restraints in the Molecular Modeling of the Binding of 6-Trifluoromethyl-7-oxo-8-Ribityllumazine (**17**) to Lumazine Synthase

| atoms  | distance (Å) |
|--|--------------|
| X (3F) <sup>a</sup> to Lys 135:NZ                              | 4.2          |
| X (3F) <sup>a</sup> to Arg127:X(NH <sub>2</sub> ) <sup>b</sup> | 5.1          |
| X (3F) <sup>a</sup> to Arg127:NE                               | 5.1          |
| X (3F) <sup>a</sup> to His88:NE2 <sup>c</sup>                  | 4.6          |
| X (3F) <sup>a</sup> to Trp22:NE1                               | 5.0          |

<sup>a</sup> The distance from the trifluoromethyl group was taken from a point at the center of the triangle represented by the three fluorine atoms.

<sup>b</sup> The distance to the two equivalent terminal Arg127 atoms was taken from a point equidistant to these two atoms. <sup>c</sup> The distance is calculated to the protonated  $\epsilon$ -nitrogen of His88, which is four bonds from the His88  $\alpha$ -carbon atom.

unassigned 100-ppm region REDOR signal (Figure 3, unassigned arrow). We tried three possibilities for the assignment: N-peptide of Lys135, His88, and Tyr89. The averaged structure after the last 10 ps was minimized (with the REDOR restraints again) to the derivative of 0.1 kcal/(mol Å<sup>2</sup>). A 10-ps run of molecular dynamics, followed by energy minimization using the five restraints in Table 1 and each of the three possible assignments (Lys135, His88, or Tyr 89 backbone nitrogens) of the 97 ppm unknown signal produced three possible models of the binding of the ligand in the active site of lumazine synthase

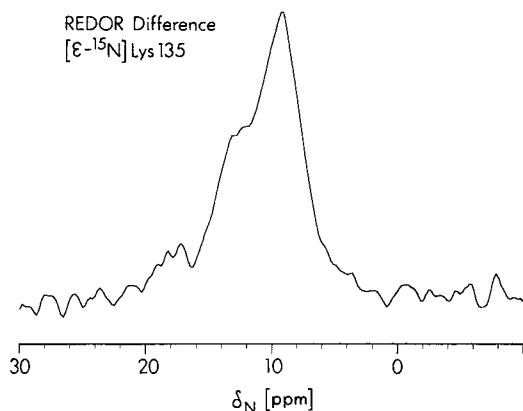


**Figure 5.** 50.7-MHz  $^{15}\text{N}\{^{19}\text{F}\}$  REDOR difference spectrum of the complex of Figure 3. This spectrum was the result of adding the difference spectra corresponding to 64, 96, and 128 rotor cycles of dipolar evolution. Only the  $\epsilon$ -nitrogen region of the spectrum is shown, which arises exclusively from Lys135. Two chemical-shift environments for this nitrogen are apparent.

(Figure 4). The model that was constructed using the backbone nitrogen of Lys135 as the restraint was deemed to be too far out of agreement with the X-ray structure, with itself because of large intrasite variations, and with the models resulting from imposition of the other restraints, and it was therefore rejected. The models resulting from the use of the backbone nitrogens of His88 and Tyr89 for the sixth restraint were in close agreement. The assignment of the 97-ppm peak to His88 was therefore arbitrarily chosen for the calculations of the final model of the binding of ligand **17** to the enzyme. The sixth restraint was taken as 4.6 Å to the  $\text{N}_\alpha$  of His88.

The five binding sites are not identical in the model of Figure 4. This is probably the result of an insufficient number of restraints on the molecular dynamics simulations. However, an expansion of the Lys135  $\epsilon$ - $^{15}\text{N}$  REDOR difference spectrum (Figure 5) indicates that there are at least two nonequivalent chemical-shift environments for this nitrogen. This observation is surprising because symmetry argues that all 60 binding sites of the lumazine synthase capsid are equivalent, at least for capsids embedded in the glassy sugar matrix of our lyophilized samples, the Lys135 side chain assumes a variety of modestly different conformations in the solid state, not unlike the heterogeneity represented by the model of Figure 4.

A representative picture of the binding of the ligand **17** to the enzyme is displayed in Figure 6. In this representation, the ligand is shown in black, and each of the nitrogen atoms used as constraints in constructing the model is highlighted in black outline. These include the indole nitrogen of Trp22, the two different types of nitrogens in the side chain of Arg127, the side-chain nitrogen atom of Lys135, and the backbone and side chain nitrogens of His88. In addition, the three fluorine atoms of the ligand that were also used in construction of the model are oversized in black.

To check that the model is self-consistent, the growth in the broad 100-ppm peak in the  $^{15}\text{N}\{^{19}\text{F}\}$  REDOR difference spectra (Figure 3, top) was calculated as a function of the number of rotor cycles and compared to experiment (Figure 7). The calculation included eight peptide nitrogens at distances of 5–8 Å from the ligand  $\text{CF}_3$  group. The prediction based on the model is in agreement with the observed results, which supports the validity of the model.

**Covalent Hydrates 15 and 16.** Next, our attention turned to the binding of the covalent hydrates **15** and **16** (epimer B and

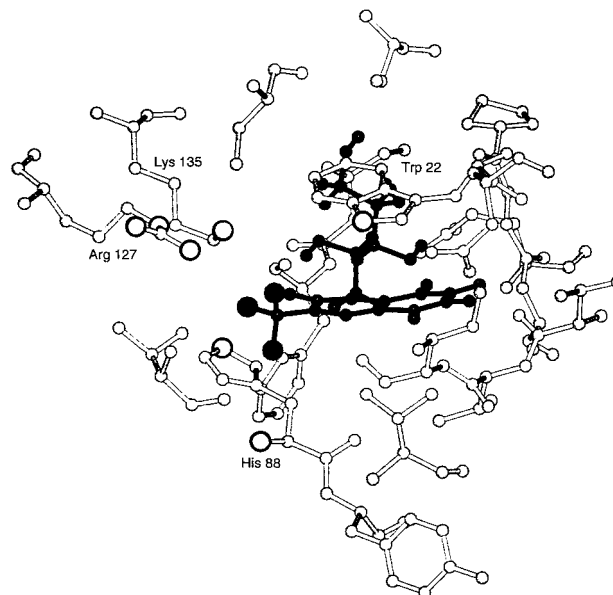


**Figure 6.** Typical arrangement of ligand and residues in the model of Figure 4 (purple). The nitrogens whose distances to the  $\text{CF}_3$  group were used as restraints in the simulation are highlighted by size and shading.

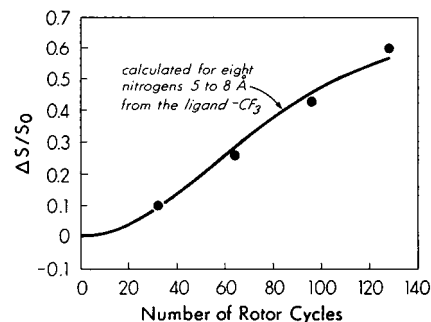


**Figure 7.** 50.7-MHz  $^{15}\text{N}\{^{19}\text{F}\}$  REDOR dephasing ( $\Delta S/S_0$ ) for all nitrogens contributing to the 100-ppm region nitrogen peak, except those of Trp22 and His88. Experimental values (solid circles) include the data of Figure 3. The solid line was calculated using distances extracted from the model of Figure 6.

epimer A) to the enzyme, and to the determination of their C-7 configurations. Previous results had shown that both epimer A and epimer B were converted nonenzymatically to **17**, and that the reaction of epimer A but not epimer B was catalyzed by lumazine synthase.<sup>29</sup> Accordingly, it was decided to study the binding of epimer B with the enzyme instead of epimer A since the complications resulting from the instability of the ligand in the presence of the enzyme could be minimized. Solid-state  $^{19}\text{F}$  NMR spectroscopy indicated that the degradation of epimer B during the preparation of solid samples of complex could be eliminated if the lyophilization were performed at  $-30^\circ\text{C}$  (Figure 8).

The 20.3-MHz  $^{15}\text{N}\{^{19}\text{F}\}$  REDOR difference spectrum of the complex of epimer B with lumazine synthase is shown in Figure 9. Comparison of the relative intensities of the Lys135 and Arg127 signals in Figure 9 with those in Figure 1 reveals that the Lys135 signal decreases in intensity and the Arg127 signal increases in intensity when epimer B is substituted for **17** as the ligand (Figure 10). This means that when epimer B is the ligand both  $\text{CF}_3$  groups are farther away from the side chain nitrogen atom of Lys135 than 4.2 Å, and at least one  $\text{CF}_3$  group is closer to the side chain nitrogens of Arg127 than 5.1 Å.

The question, then, is whether the Lys135 and Arg127 nitrogens would be closer to or farther away from the fluorines

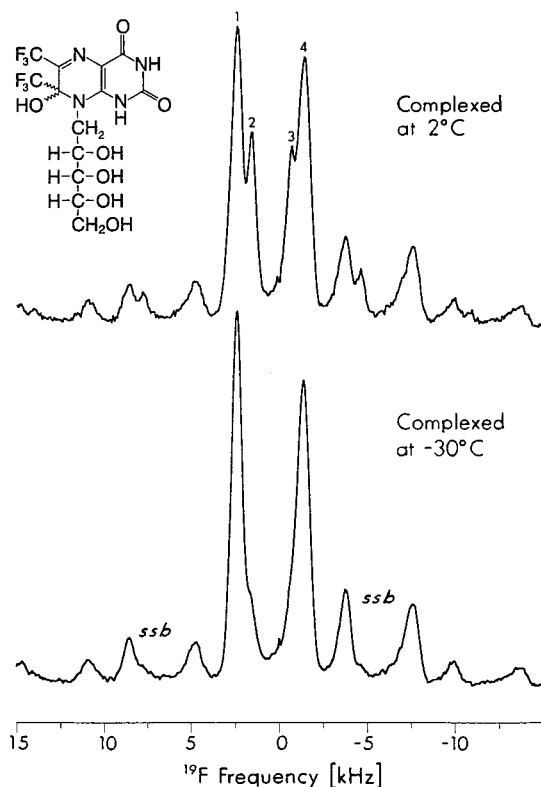


**Figure 8.** 188-MHz  $^{19}\text{F}$  cross-polarization magic-angle spinning NMR spectra of one of the epimers of 6,7-bis(trifluoromethyl)-8-ribityllumazine complexed to [uniform- $^{15}\text{N}$ ]-F22W-lumazine synthase as a function of the temperature for the formation of the complex. Only two major lines (1 and 4) are observed in the bottom spectrum indicating that complex formation by low-temperature trapping, followed by low-temperature lyophilization, avoided degradation; the minor lines arise from the 6.250-kHz magic-angle spinning. The additional lines in the top spectrum (lines 2 and 3) indicate chemical modification of the epimer.

when the two structures **15** and **16** occupy the active site of the enzyme. An answer to this question would allow the assignment of the absolute configurations to epimers A and B. Therefore, the structures of both **15** and **16** were overlapped with the structures of **17** in five of the active sites surrounding an enzyme pentamer (Figure 4). In each case (**15** or **16**), energy minimization followed in two steps. First, the protein was fixed and the energy of the bis(trifluoromethyl) compound (**15** or **16**) was minimized. Then, everything was unfrozen (no restraints) and the energy re-minimized. A 10-ps equilibration followed by a 10-ps dynamics simulation were performed with two restraints: the 4.6-Å distances from the protonated  $\epsilon$  ring nitrogen and N-peptide nitrogen of His88 to the C-6 trifluoromethyl group. The backbone was tethered, and the average structures after the 10-ps dynamics run were minimized with the two restraints described above. The distances to each of the two trifluoromethyl groups were then calculated to the relevant nitrogens of Lys135 and Arg127 at each of the five sites, and the results are listed in Table 2.

Because there are two trifluoromethyl groups and two Arg127 nitrogen atoms contributing to the distance calculations in each site, there are four distances calculated between fluorine and Arg127 nitrogen at each site. The calculations are based on modeling at five active sites surrounding one pentamer of lumazine synthase, so there are a total of twenty distance calculations that can be considered as contributing to the intensity of the Arg127 REDOR difference signal. Each of these twenty distances is listed in Table 2. It can be seen that nine of

**Table 2.** Distances Calculated for Compounds **15** and **16** in Five of the Active Sites of Lumazine Synthase

| atoms   | distance (Å) <sup>a</sup> at site |     |     |     |     |
|---|-----------------------------------|-----|-----|-----|-----|
|   | 1                                 | 2   | 3   | 4   | 5   |
| structure <b>15</b> :   |                                   |     |     |     |     |
| 6X (3F) <sup>b</sup> to Arg127:X(NH <sub>2</sub> ) <sup>c</sup> | 6.0                               | 5.2 | 4.7 | 4.4 | 7.6 |
| 6X (3F) <sup>b</sup> to Arg127:NE                               | 5.0                               | 4.7 | 4.9 | 5.2 | 6.1 |
| 7X (3F) <sup>d</sup> to Arg127:X(NH <sub>2</sub> ) <sup>c</sup> | 7.2                               | 4.9 | 6.8 | 4.9 | 9.3 |
| 7X (3F) <sup>d</sup> to Arg127:NE                               | 5.6                               | 5.0 | 7.4 | 5.0 | 7.5 |
| 6X (3F) <sup>b</sup> to Lys135:NZ                               | 4.5                               | 5.2 | 5.0 | 5.4 | 4.7 |
| 7X (3F) <sup>b</sup> to Lys135:NZ                               | 4.1                               | 4.3 | 3.7 | 3.2 | 4.6 |
| structure <b>16</b> :   |                                   |     |     |     |     |
| 6X (3F) <sup>b</sup> to Arg127:X(NH <sub>2</sub> ) <sup>c</sup> | 6.8                               | 7.3 | 4.1 | 4.8 | 7.4 |
| 6X (3F) <sup>b</sup> to Arg127:NE                               | 5.3                               | 6.6 | 4.5 | 5.8 | 6.1 |
| 7X (3F) <sup>d</sup> to Arg127:X(NH <sub>2</sub> ) <sup>c</sup> | 8.0                               | 8.4 | 5.8 | 4.3 | 8.0 |
| 7X (3F) <sup>d</sup> to Arg127:NE                               | 6.5                               | 7.1 | 6.5 | 4.9 | 6.8 |
| 6X (3F) <sup>b</sup> to Lys135:NZ                               | 4.4                               | 5.4 | 4.4 | 5.8 | 4.7 |
| 7X (3F) <sup>b</sup> to Lys135:NZ                               | 5.6                               | 4.7 | 5.0 | 3.4 | 4.4 |

<sup>a</sup> The distances listed to Lys135 are accurate to within  $\pm 0.2$  Å. The other distances are accurate to within  $\pm 0.4$  Å. <sup>b</sup> The distance was calculated from the center of the triangle represented by the three fluorine atoms of the C-6 trifluoromethyl group. <sup>c</sup> The distance to the two equivalent terminal Arg127 atoms was taken from a point equidistant to these two atoms. <sup>d</sup> The distance was calculated from the center of the triangle represented by the three fluorine atoms of the C-7 trifluoromethyl group.

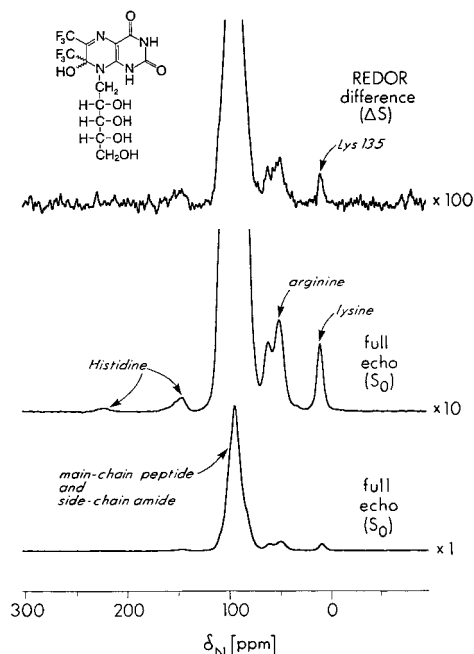


**Figure 9.** 20.3-MHz  $^{15}\text{N}\{^{19}\text{F}\}$  REDOR NMR spectra of 6,7-bis(trifluoromethyl)-8-ribityllumazine complexed to [uniform- $^{15}\text{N}$ ]-F22W-lumazine synthase after 96 rotor cycles of dipolar evolution with magic-angle spinning at 5.555 kHz. This spinning speed was chosen to satisfy the CEDRA ( $n = 1$ ) condition for the two fluorine resonances of the ligand and so suppress the effects of  $^{19}\text{F}$ - $^{19}\text{F}$  coupling. The 17-ms of dipolar evolution is close to the 12.4-ms of evolution for the REDOR experiment of Figure 1. The lysine difference peak is reduced in intensity and the arginine difference peaks increased, relative to those of Figure 1.

the twenty distances are less than 5.1 Å (the distance calculated from the Arg127 side chain nitrogens to the trifluoromethyl group of **17**) for structure **15**, but only five of the distances are less than 5.1 Å for structure **16**. Because the REDOR data indicate that, overall, the fluorine of the ligand is closer to the side chain nitrogens in epimer B than it is in inhibitor **17**, epimer B could be tentatively assigned structure **15**.

A second line of reasoning involves the distances between the terminal nitrogen of Lys135 and the trifluoromethyl group

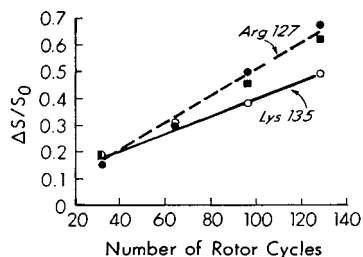


**Figure 10.** 20.3-MHz  $^{15}\text{N}\{^{19}\text{F}\}$  REDOR dephasing ( $\Delta S/S_0$ ) for three of the nitrogen peaks of the complex of Figure 9.

of the ligand. One would expect that the model (**15** vs **16**) that shows a greater distance between fluorine and the terminal nitrogen of Lys135 would be more consistent with the data. Since there are two trifluoromethyl groups of the ligand, there are two distance calculations, one from each trifluoromethyl group to the terminal nitrogen atom of Lys135. Because five of the possible sixty active sites of lumazine synthase are used in the modeling (Figure 4), there are a total of 10 distance calculations that can be considered. It can be seen from Table 2 that seven of these distances are greater than 4.2 Å for structure **15**, which is the distance from the trifluoromethyl group of **17** to the terminal nitrogen atom of Lys135 (Table 1). On the other hand, nine of these distances are calculated to be greater than 4.2 Å for structure **16**. Although this would argue that epimer B has structure **16**, which is the opposite conclusion reached on the basis of the measurements to Arg127, we consider the differences between the models involving Arg 127 to be more significant. In short, we feel that both structures are consistent with the Lys135 requirement but only one is consistent with the Arg127 requirement.

Admittedly, this reasoning is complicated and somewhat speculative, and therefore additional evidence was sought that would corroborate the conclusions based on signal intensities in the REDOR data. Because there is a stereoselective catalysis of the conversion of epimer A but not epimer B to the 7-oxo compound **17** by lumazine synthase, a conclusion about the stereochemistry of the ligand might possibly be reached by determining which diastereomer would position the 7-hydroxy group near a basic residue in the enzyme that would facilitate the fluoroform elimination reaction by accepting a proton from the substrate.<sup>29</sup> The distances to each of the nonequivalent nitrogens of Arg 127, the side-chain nitrogen of Lys 135, and the unprotonated His88 imidazole nitrogen were calculated at each site of the two model structures. The results of these calculations for each of the two epimers **15** and **16** are listed in Table 3. It is evident that there are two of the four possible basic nitrogens that are located close enough to the C-7 hydroxyl group to be able to facilitate deprotonation: the terminal nitrogen on the Lys135 side chain and the unprotonated imidazole nitrogen of His88. Furthermore, the hydroxyl group of the substrate is positioned close enough to these nitrogens in structure **16**, but not structure **15**, for the assumed proton abstraction to occur. On the basis of this evidence, it may be concluded that epimer A has the 7R structure **16**, and therefore epimer B has the 7S structure **15** (Figure 11).

The assignment of the epimer A (**16**) and epimer B (**15**) structures is important because of the proposed involvement of the related substance **9** in the reactions catalyzed by both lumazine synthase and riboflavin synthase (Schemes 2 and 3). Prior studies have shown that only epimer A (**16**), and not epimer B (**15**), binds to the light riboflavin synthase of *Bacillus subtilis*.<sup>28</sup> On the basis of the present results, it seems logical to assume that only the epimer of **9** which resembles epimer A

**Table 3.** Distances Calculated from the C-7 Hydroxyl Group Oxygen of **15** and **16** to the Side Chain Nitrogen Atoms of Arg127, Lys135, and the Unprotonated Imidazole Nitrogen of His88 in Five Active Sites of Lumazine Synthase

| atoms                 | distance (Å) | atoms              | distance (Å) |
|-----------------------|--------------|--------------------|--------------|
| structure <b>15</b>   |              |                    |              |
| 7O_1 to Arg127C:N2    | 7.2          | 7O_1 to Lys135C:NZ | 6.6          |
| 7O_1 to Arg127C:N1    | 8.9          | 7O_2 to Lys135E:NZ | 6.9          |
| 7O_2 to Arg127E:N2    | 4.0          | 7O_3 to Lys135D:NZ | 3.1          |
| 7O_2 to Arg127E:N1    | 5.8          | 7O_4 to Lys135A:NZ | 6.0          |
| 7O_3 to Arg127D:N2    | 4.3          | 7O_5 to Lys135B:NZ | 6.9          |
| 7O_3 to Arg127D:N1    | 4.2          | 7O_1 to His88B:ND1 | 6.7          |
| 7O_4 to Arg127A:N2    | 5.4          | 7O_2 to His88C:ND1 | 6.7          |
| 7O_4 to Arg127A:N1    | 5.8          | 7O_3 to His88E:ND1 | 6.3          |
| 7O_5 to Arg127B:N2    | 9.3          | 7O_4 to His88D:ND1 | 6.4          |
| 7O_5 to Arg127B:N1    | 10.7         | 7O_5 to His88A:ND1 | 7.4          |
| structure <b>16</b> : |              |                    |              |
| 7O_1 to Arg127C:N2    | 8.5          | 7O_1 to Lys135C:NZ | 3.9          |
| 7O_1 to Arg127C:N1    | 9.3          | 7O_2 to Lys135E:NZ | 4.6          |
| 7O_2 to Arg127E:N2    | 8.0          | 7O_3 to Lys135D:NZ | 3.6          |
| 7O_2 to Arg127E:N1    | 9.6          | 7O_4 to Lys135A:NZ | 4.2          |
| 7O_3 to Arg127D:N2    | 7.1          | 7O_5 to Lys135B:NZ | 5.4          |
| 7O_3 to Arg127D:N1    | 7.0          | 7O_1 to His88B:ND1 | 4.0          |
| 7O_4 to Arg127A:N2    | 5.8          | 7O_2 to His88C:ND1 | 3.7          |
| 7O_4 to Arg127A:N1    | 7.1          | 7O_3 to His88E:ND1 | 5.0          |
| 7O_5 to Arg127B:N2    | 8.6          | 7O_4 to His88D:ND1 | 4.3          |
| 7O_5 to Arg127B:N1    | 9.8          | 7O_5 to His88A:ND1 | 4.6          |

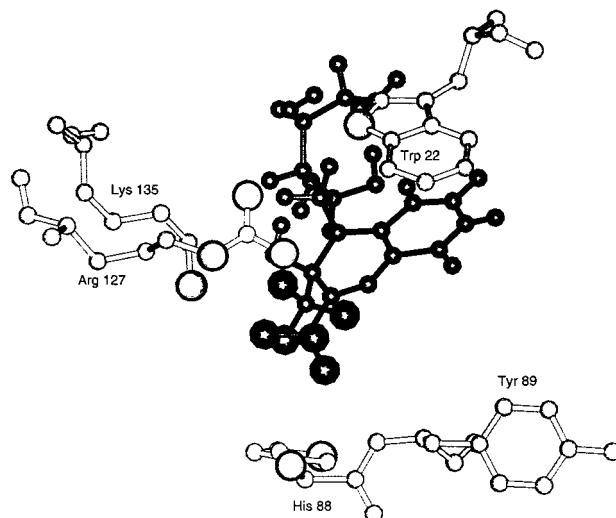


**Figure 11.** Arrangement of ligand structure **15** and proximate residues of lumazine synthase for the model of Tables 2 and 3.

(**16**) would serve as a substrate for riboflavin synthase. Moreover, it has been established that lumazine synthase catalyzes the elimination of fluoroform from epimer A (**16**) and not from epimer B (**15**).<sup>29</sup> It now appears that this reflects a stereoselective proton abstraction by either Lys135 or His88 from the C-7 hydroxyl group of epimer A (**16**) but not epimer B (**15**) (Figure 11). Studies with lumazine synthase mutants have shown that the  $^{19}\text{F}$  NMR chemical shift of the C-7 trifluoromethyl group of epimer B (**15**) is very sensitive to the identity of the amino acid residue present at position 22.<sup>5</sup> It seems logical from inspection of Figure 11 that this may reflect the modulation of the positioning of the C-7 trifluoromethyl group of epimer B (**15**) relative to the imidazole ring of His88 by the amino acid residue present at position 22. In other words, the amino acid residue at position 22 exerts a nonbonded interaction on the lumazine ring, and changing it could alter the position of the C-7 trifluoromethyl group in epimer B (**15**) relative to the imidazole ring of His88. The structure of the complex in Figure



11 is also significant because it provides information about how the hypothetical intermediate **9** (Scheme 2) is bound in the active site during the reaction catalyzed by lumazine synthase.

The present investigation demonstrates the utility of REDOR NMR as a tool for the investigation of protein–ligand complexes in general. The development of these techniques could have major significance for structural and mechanistic enzymology, and it is also of obvious importance for medicinal chemistry research. The high-resolution structure of lumazine synthase resulting from the present study is currently being employed in the design of metabolically stable analogues of hypothetical intermediates in the enzyme-catalyzed reaction pathway that will serve as effective enzyme inhibitors and will also provide information about the structures of the enzyme-bound intermediates and the active site during catalysis. For example, metabolically stable phosphonate analogues of the hypothetical phosphate intermediate **6** have been synthesized<sup>31</sup> and are presently being utilized in conjunction with X-ray crystallography and REDOR NMR to provide information about the conformation of **6** when bound in the active site of lumazine synthase.

## Experimental Section

**(7R)-6,7-Bis(trifluoromethyl)-7-hydroxy-8-D-ribityllumazine (15) and 6-Trifluoromethyl-7-oxo-8-D-ribityllumazine (17).** These compounds were prepared as described previously.<sup>27,28</sup>

**The Uniformly <sup>15</sup>N-Labeled F22W Mutant of *B. subtilis* Lumazine Synthase.** The construction of the plasmid pNCO-ribH-F22W directing the hyperexpression of the gene specifying the F22W mutant of *B. subtilis* will be described elsewhere (M. Fischer et al., manuscript in preparation). The plasmid was transduced into *E. coli* strain XL1 yielding strain XL1-p602-BS-ribH-F22W. The recombinant strain was grown in M9 medium (Sambrook, J., Fritsch, E. F., Mannatis, T. *Molecular Cloning. A Laboratory Manual*, 2nd ed.; Cold Spring Harbor Laboratory Press, 1989) containing 0.7 g of <sup>15</sup>NH<sub>4</sub>Cl per liter as the only source of nitrogen. IPTG (final concentration, 2 mM) was added to cultures during shaking when they had reached an optical density of 0.7 (600 nm). Incubation was continued for 5 h. The cells were harvested by centrifugation. Lumazine synthase was purified as described earlier.<sup>32</sup>

**Preparation of the Complex of the <sup>15</sup>N-Labeled Lumazine Synthase-F22W Mutant with 6-Trifluoromethyl-7-oxo-8-ribityllumazine (17).** Uniformly <sup>15</sup>N-labeled lumazine synthase-F22W (100 mg), in the 60-mer capsid form, was complexed 1:1 in a lyophilization flask with **17** at 2 °C and then at –5 °C in 50 mL of 50 mM triethanolamine–HCl, pH 7.2, containing 10 mM trehalose, and 0.05% PEG 8000. The final concentration of protein subunit and ligand was 136 μM. The supercooled solution was frozen by lowering the bath temperature to –8 °C and then to –60 °C before the flask was attached to a 5 mTorr vacuum for lyophilization. NMR revealed about 75% occupancy, indicating the ligand **17** had a K<sub>D</sub> of about 40 μM for lumazine synthase under these binding conditions. After a series of NMR experiments, this sample was rehydrated in 50 mM triethanolamine–HCl, pH 7.2. Buffer exchange was effected by four rounds of volume reduction from 50 to 8 mL in this buffer via ultrafiltration against a TM-10 (MWCO = 10 kD) filter. Eighty-five milligrams was recovered after denatured protein was removed by centrifugation. The volume was adjusted to 10 mL in 50 mM triethanolamine–HCl, 30 mM trehalose, and 0.25%

PEG 8000, pH 7.2. At this dilution, the occupancy should have been approximately 93%. This sample was then frozen and lyophilized for NMR experiments at higher field.

**Preparation of the Complex of <sup>15</sup>N-Labeled Lumazine Synthase-F22W Mutant with (7S)-6,7-Bis(trifluoromethyl)-7-hydroxy-8-ribityllumazine (15, Epimer B).** Using a method developed in our laboratory for trapping and stabilizing enzyme substrates in a lyophilized matrix,<sup>30</sup> the unstable epimer B was successfully complexed to lumazine synthase without evidence of significant degradation. Uniformly <sup>15</sup>N-labeled lumazine synthase-F22W (100 mg) was exchanged into 50 mM triethanolamine–formate, pH 6.0, containing 35% methanol as an antifreeze reagent, 30 mM trehalose as a lyoprotectant, and 0.4% PEG 8000 (w/v) as a cryoprotectant. The solution, in a lyophilization flask, was then placed in a –25 °C bath until equilibrated. An equimolar amount of epimer B, dissolved in methanol, was added to this fluid –25 °C mixture. After being mixed by swirling, the solution was incubated for 10 min at –25 °C and then rapidly frozen in liquid nitrogen. The flask was attached to a 5 mTorr vacuum and placed in a –80 °C bath. Lyophilization was accomplished by keeping the external flask temperature at subzero temperatures throughout the primary drying phase thereby stabilizing the unstable substrate in a solid matrix. When the rate of sublimation decreased, as measured by a vacuum sensor mounted near the flask, the bath temperature was gradually raised to remove any residual water.

**REDOR NMR.** <sup>15</sup>N{<sup>19</sup>F} REDOR was performed using a 6-frequency transmission-line probe having a 12-mm long, 6-mm inside-diameter analytical coil and a Chemagnetics/Varian ceramic stator. Powdered samples were contained in thin-wall Chemagnetics/Varian 5-mm outside diameter zirconia rotors. The rotors were spun at 6250 Hz with the speed under active control to within ±2 Hz. The spectrometer was controlled by a Tecmag pulse programmer. <sup>15</sup>N radio frequency pulses (50.7 MHz) were produced by a 2-kW American Microwave Technology power amplifier. <sup>1</sup>H (500 MHz) and <sup>19</sup>F (470 MHz) radio frequency pulses were generated by 1-kW Creative Electronics tube amplifiers driven by 100-W American Microwave Technology power amplifiers. The  $\pi$  pulse lengths were 10 μs for <sup>15</sup>N and 5 μs for <sup>19</sup>F. Distance measurements using <sup>19</sup>F dephasing were calibrated using the two-bond coupling of [<sup>19</sup>F]polycarbonate. Standard XY-8 phase cycling was used for REDOR. A 12-T static magnetic field was provided by an 89-mm bore Magnex superconducting solenoid. Proton–carbon cross-polarization transfers were made in 2 ms at 50 kHz. Proton dipolar decoupling was 100 kHz during data acquisition. Nitrogen chemical shifts were referenced relative to external solid ammonium sulfate. REDOR experiments performed at 4.7 T involved a spectrometer and 4-frequency transmission-line probe described earlier.<sup>21</sup>

**Molecular Modeling.** Computational results were obtained using software programs from MSI of San Diego; dynamics calculations were done with the Discover-3 program, using the CVFF force field. Dynamics runs were performed in 0.5-fs steps. A constant-temperature, constant-volume ensemble with velocity scaling for temperature controlling was used. The system was equilibrated for 10 ps to the target temperature of 300 K and the data were collected for 10–20 ps, averaged every 100 fs.

**Acknowledgment.** This work was supported by NIH grants GM-40634 (J.S.) and GM51469 (M.C.), as well as by support from the Deutsche Forschungsgemeinschaft and Fonds der Chemischen Industrie (A.B.). The 6-frequency transmission-line probe was designed and built by R. A. McKay (Washington University) supported by NIH grant RR09974, together with a spectrometer also built by R. A. McKay, supported by NSF grant BIR9400072.

JA983792U

(31) Cushman, M.; Mihalic, J. T.; Kis, K.; Bacher, A. *J. Org. Chem.* **1999**, *64*, 3838–3845.

(32) Bacher, A.; Eberhardt, S.; Fischer, M.; Mörtl, S.; Kis, K.; Kugelbrey, K.; Scheuring, J. In *Methods Enzymology*; McCormick, D. B., Suttie, J. W., Wagner, C., Eds.; Academic Press: San Diego, 1997; Vol. 280, pp 389–399.